Computer Assisted Mechanics and Engineering Sciences, 10: 23–31, 2003.

The biomechanics of atherosclerosis development

Oluwole D. Makinde
Applied Mathematics Department, University of the North
P/Bag X1106, Sovenga 0727, Republic of South Africa

Thomas M. Acho
Mathematics Department, Vista University
P.O. Box 380, Bloemfontein 9300, Republic of South Africa

Precious Sibanda
Mathematics Department, University of Zimbabwe
P.O. Box MP 167, Harare, Zimbabwe

Edward M. Lungu
Mathematics Department, University of Botswana
Private Bag 0022, Gaborone, Botswana

(Received November 6, 2000)

In this paper, we investigate the bio-mechanics of atherosclerosis development in human physiology. Blood is modelled as an incompressible fluid of variable viscosity flowing in a slightly diverging channel (i.e. large artery) of small aspect ratio [15]. The hypothetical viewpoint in this work is the existence of relationship between the atherosclerosis development, blood viscosity, flow separation and turning points in the flow field. The problem is tackled by asymptotic approximation and the graphical results are discussed quantitatively.

Keywords: aorta, blood viscosity, bifurcation study, atherosclerosis development

1. Introduction

Atherosclerosis is a common disorder of the arteries in which fatty material is deposited in the vessel wall, resulting in narrowing and eventual impairment of blood flow. Cerebrovascular disease, peripheral vascular disease, high bloods pressure and kidney disease involving dialysis are also disorders that may be associated with atherosclerosis. The arterial blood flow provides a way for glucose, oxygen and hormones to reach various organs around the body. Blood is a suspension of cells in plasma and can be separated into microscopically visible elements and liquid plasma. The elements are red cells or erythrocytes, the white cells or leukocytes, and the platelets or thrombocytes. It is very evident that blood viscosity depends largely on its composition. In the large blood vessels it is a good approximation to consider whole blood as a Newtonian viscous fluid [10]. Blood viscosity and its major determinants such as plasma viscosity, fibrinogen (a protein involved in clotting) and red cell volume (hematocrit), may be important risk factors for the early development of atherosclerosis. The process starts from the build-up of cholesterol, fats and biological debris in the tissue lining the inside of blood vessels. This build-up can obstruct blood flow to the heart and brain and thereby cause heart attack or stroke. Recently, Lee [9] conducted a bio-statistical survey and concluded that

blood viscosity is related to risk of early atherosclerosis in [8] indicate that in the arterial systems static zones occur, which are due to separation of the main flow from the walls of the arteries. It is suggested that in these separation zones there is an interaction of platelets and fibrinogen to form a mesh in which lipid particles become trapped, with the subsequent formation of a plaque of atheroma. Certain thrombus formation is one of the major complications of prosthetic heart valves, and many investigators have suggested that stagnation zones near the valve contribute to the formation of thrombi.

Mathematically speaking, several authors, e.g. [3, 4, 11, 12, 14, 16–21, etc.], have studied such flows with reference to physiological situations. In all these studies, the existence of separation in the flow field is observed and blood viscosity is taken as constant. However, in many situations, the blood viscosity varies due to elevated level of certain blood substances and this variation in blood viscosity is certainly going to affect the general flow structure as well as the bifurcation that occur in the flow field as the flow Reynolds number increases including the internal flow separation which ultimately may lead to early development of atherosclerosis disease.

The complexity of the dynamics of arterial blood flow made it very difficult to handle mathematically with a single model. For instant, the deformability of arterial wall, the unusual pulsatility of the flow, non-uniform blood viscosity, absorption of nutrients through arterial wall, etc., contributed to its mathematical complexity. However, in the present paper, we shall improve on the steady flow analysis of [14, 17] by including variable blood viscosity and the bifurcation study. Our objective is to demonstrate the intimacy that exist between the blood viscosity, flow field turning points and atherosclerosis development. We employed the technique of extending a regular perturbation series to high order by computer, and then analysing the coefficients to reveal the structure of the solution [6]. In the following sections, the problem is formulated, analysed, solved and discussed.

2. Mathematical formulation

In the large arteries, we regard blood as an incompressible fluid with variable viscosity [18]. It is assumed that the flow is fully developed and the blood vessel is modelled as a two-dimensional symmetrical channel. Take a Cartesian co-ordinate system (x, y) where $0x$ lies along the centre of the artery, and y is the distance measured in the transverse direction. Let u and v be the velocity components in the directions of x and y increasing respectively, $a(x)$ defines the arterial wall geometry. Following [8], the continuity and Navier–Stokes equations governing the flow are

$$\frac{\partial v}{\partial y} + \frac{\partial u}{\partial x} = 0, \tag{1}$$

$$\rho\left(u\frac{\partial u}{\partial x} + v\frac{\partial u}{\partial y}\right) = -\frac{\partial P}{\partial x} - \left(\frac{\partial \sigma_{yx}}{\partial y} + \frac{\partial \sigma_{xx}}{\partial x}\right), \tag{2}$$

$$\rho\left(u\frac{\partial v}{\partial x} + v\frac{\partial v}{\partial y}\right) = -\frac{\partial P}{\partial y} - \left(\frac{\partial \sigma_{yy}}{\partial y} + \frac{\partial \sigma_{yx}}{\partial x}\right), \tag{3}$$

where σ_{yy}, σ_{xx}, σ_{xy} are the usual stress components, i.e.

$$\sigma_{xy} = -\mu\left(\frac{\partial u}{\partial y} + \frac{\partial v}{\partial x}\right), \qquad \sigma_{yy} = -2\mu\frac{\partial v}{\partial y}, \qquad \sigma_{xx} = -2\mu\frac{\partial u}{\partial x}, \tag{4}$$

and μ is the blood dynamic viscosity defined as

$$\mu = \mu_0\left[1 + \frac{(\alpha - 1)y}{a_0}\right], \tag{5}$$

P is the blood pressure, ρ the blood density, α the blood viscosity variation coefficient such that $\alpha = 1$ corresponds to the case of uniform blood viscosity, μ_0 is the blood reference dynamic viscosity,

and a_0 is the arterial characteristic half width. In Eq. (5), we have assumed a small transverse variation in the blood viscosity i.e. between the arterial inner wall and the center region of the artery. This assumption is physiologically justify in the large artery, since the concentration of red blood cells seem to be higher near the arterial inner wall where the exchange of oxygen and nutrient to the body tissue takes place [18]. The appropriate boundary conditions are

1. Symmetric condition along the arterial centreline i.e.

$$\frac{\partial u}{\partial y} = 0, \quad v = 0 \qquad \text{on } y = 0. \tag{6}$$

2. There is no tangential fluid motion at the wall i.e.,

$$u + v\frac{\partial a}{\partial x} = 0 \qquad \text{on } y = a(x). \tag{7}$$

The fluid flux across any cross-section of the artery is described as

$$Q = \int_0^{a(x)} u \, dy. \tag{8}$$

The arterial half width ($y = a(x) = a_0 S(x/L)$) is assumed to vary slowly with axial distance such that $0 < \delta = a_0/L \ll 1$, and L is the characteristic length. We introduce the stream-function Ψ and vorticity ω in the following manner,

$$u = \frac{\partial \Psi}{\partial y} \qquad \text{and} \qquad v = -\frac{\partial \Psi}{\partial x}, \tag{9}$$

$$\omega = \frac{\partial v}{\partial x} - \frac{\partial u}{\partial y} = -\frac{\partial^2 \Psi}{\partial x^2} - \frac{\partial^2 \Psi}{\partial y^2}. \tag{10}$$

Eliminating pressure P from Eqs. (2) and (3) and using Eqs. (5), (9) and (10) we get

$$\frac{\partial(\omega, \Psi)}{\partial(x, y)} = \nu_0 \left[1 + \frac{(\alpha - 1)y}{a_0}\right] \nabla^2 \omega + \nu_0 \frac{(\alpha - 1)}{a_0} \left[\frac{\partial \omega}{\partial y} - \nabla^2\left(\frac{\partial \Psi}{\partial y}\right)\right], \tag{11}$$

$$\omega = -\nabla^2 \Psi, \tag{12}$$

$$\frac{\partial^2 \Psi}{\partial y^2} = 0, \quad \Psi = 0 \qquad \text{on } y = 0, \tag{13}$$

$$\frac{\partial \Psi}{\partial y} = \frac{\partial \Psi}{\partial x}\frac{\partial a}{\partial x}, \quad \Psi = Q \qquad \text{on } y = a(x/L), \tag{14}$$

where $\nu_0 = \mu_0/\rho$ is the blood reference kinematic viscosity coefficient. The following dimensionless variables are introduced,

$$\omega' = \frac{a_0^2 \omega}{Q}, \qquad x' = \frac{\delta x}{a_0}, \qquad y' = \frac{\delta y}{a_0}, \qquad \Psi' = \frac{\Psi}{Q}. \tag{15}$$

The arterial aspect ratio is very small, hence we can neglect terms of order δ^2 and higher power in the dimensionless governing equations. We obtain (neglecting primes for clarity),

$$\frac{\partial^2 \omega}{\partial y^2} = Re\left[\frac{\partial(\omega, \Psi)}{\partial(x, y)} - \beta\left(y\frac{\partial^2 \omega}{\partial y^2} + 2\frac{\partial \omega}{\partial y}\right)\right], \tag{16}$$

$$\omega = -\frac{\partial^2 \Psi}{\partial y^2}, \tag{17}$$

$$\Psi = 0, \quad \frac{\partial^2 \Psi}{\partial y^2} = 0 \qquad \text{on } y = 0, \tag{18}$$

$$\frac{\partial \Psi}{\partial y} = 0, \quad \Psi = 1 \qquad \text{on } y = S, \tag{19}$$

where $Re = Qa_0/L\nu_0$ and $\beta = (\alpha - 1)\nu_0 L/a_0 Q$ are the flow Reynolds number and the blood viscosity variation parameter respectively.

3. Perturbation Expansion

The problem posed by Eqs. (16)–(19) is non-linear and therefore not amenable to analytical treatment. For low Reynolds number flow, we shall seek asymptotic expansion of the form

$$\Psi = \sum_{i=0}^{\infty} Re^i \Psi_i\,, \qquad \omega = \sum_{i=0}^{\infty} Re^i \omega_i\,. \tag{20}$$

Substituting the above expressions (20) into (16)–(19) and collecting the coefficients of like powers of Re we obtained and solved the equations governing Ψ and ω as follows,

Zeroth Order:

$$\frac{\partial^2 \omega_0}{\partial y^2} = 0, \qquad \omega_0 = -\frac{\partial^2 \Psi_0}{\partial y^2}\,, \tag{21}$$

$$\Psi_0 = 0, \quad \frac{\partial^2 \Psi_0}{\partial y^2} = 0 \qquad \text{on } y = 0, \tag{22}$$

$$\frac{\partial \Psi_0}{\partial y} = 0, \quad \Psi_0 = 1 \qquad \text{on } y = S. \tag{23}$$

Higher Order ($n \geq 1$):

$$\frac{\partial^2 \omega_n}{\partial y^2} = \sum_{i=0}^{n-1} \frac{\partial(\omega_i\,,\, \Psi_{n-1-i})}{\partial(x, y)} - \beta \left(y \frac{\partial^2 \omega_{n-1}}{\partial y^2} + 2 \frac{\partial \omega_{n-1}}{\partial y} \right), \tag{24}$$

$$\omega_n = -\frac{\partial^2 \Psi_n}{\partial y^2}\,, \tag{25}$$

$$\Psi_n = 0, \quad \frac{\partial^2 \Psi_n}{\partial y^2} = 0 \qquad \text{on } y = 0, \tag{26}$$

$$\frac{\partial \Psi_n}{\partial y} = 0, \quad \Psi_n = 0 \qquad \text{on } y = S. \tag{27}$$

Since it seems cumbersome to obtain many terms of the solution series manually, we have written a MAPLE program that calculates successively the coefficients of the solution series. In outline, it consists of the following segments:

(i) Declaration of arrays for the solution series coefficients. $\Psi = \text{array}(0..30)$, $\omega = \text{array}(0..30)$

(ii) Input the leading order term and their derivatives (i.e. solution of Eqs. (21)–(23)).

(iii) Input the modelled arterial geometry slope (i.e. $\mathrm{d}S/\mathrm{d}x$).

(iv) Using a MAPLE loop procedure, iterate to solve Eqs. (24)–(27) for the higher order terms.

(v) Compute the wall shear stress and the axial pressure gradient.

Some of the solution for stream-function and vorticity obtained initially manually and also by using the above MAPLE procedure are then given as follows,

$$\Psi = -\frac{1}{2}(\eta^3 - 3\eta) - \frac{3ReS_x}{280}(\eta^7 - 7\eta^5 + 11\eta^3 - 5\eta) + \frac{ReS\beta}{8}(2\eta^4 - 3\eta^3 + \eta) + \cdots, \tag{28}$$

$$\omega = \frac{3\eta}{S^2} + \frac{3ReS_x}{140S^2}(21\eta^5 - 70\eta^3 + 33\eta) - \frac{3Re\beta}{4S}(4\eta^2 - 3\eta) + \cdots, \tag{29}$$

where S_x represents the derivative of S with respect to x and $\eta = y/S$. The shear stress at the wall of the artery is given by

$$\tau_w = -\frac{1}{(1+a_x^2)}\left[(\sigma_{yy} - \sigma_{xx})a_x + (1+a_x^2)\sigma_{xy}\right] \qquad \text{on } y = a(x/L), \tag{30}$$

where where σ_{yy} , σ_{xx} , σ_{xy} are the usual stress components, i.e.

$$\sigma_{xy} = \mu(\Psi_{yy} - \Psi_{xx}), \qquad \sigma_{yy} - \sigma_{xx} = -4\mu\Psi_{xy}\,. \tag{31}$$

The subscripts (x, y) denote partial differentiation with respect to (x, y), respectively. The dimensionless form of wall shear stress can be written as

$$G = \frac{a_0^2 S^2}{\mu Q}\tau_w = -\frac{S^2}{(1+\delta^2 S_x^2)}\left[(\Psi_{yy} - \delta^2\Psi_{xx})(1+\delta^2 S_x^2) - 4\delta^2 S_x\Psi_{xy}\right] \tag{32}$$

and we obtain

$$G = 3 - \frac{12S_xRe}{35} - \frac{3S\beta Re}{4} + \cdots \qquad \text{on } y = S. \tag{33}$$

From axial component of the Navier–Stokes equation (2), we can determine the blood pressure distribution. The solution for the pressure field is taken as

$$P = \frac{\mu Q}{a^2}q \tag{34}$$

where q is given as

$$q = \frac{1}{\delta}P_0 + P_1 + \delta P_2 + O(\delta^2) + \cdots. \tag{35}$$

The blood pressure gradient in the longitudinal direction is given as

$$\frac{\partial q}{\partial x} = \frac{1}{\delta}\Delta P = \frac{1}{\delta S^3}\left\{-3 + \left[\frac{54S_x}{35} + \frac{3(140y - 105S)\beta}{140}\right]Re + \cdots\right\}. \tag{36}$$

The solution for the pressure field is

$$q = \frac{1}{\delta}\int_0^x \nabla P\,\mathrm{d}x. \tag{37}$$

4. Computer extension and bifurcation study

We shall assume a linearly diverging arterial geometry defined by $S = 1 + mx$, where $0 < m \ll 1$ represent the arterial slope. This is valid in the large artery especially near the aortic valve, as the heart pumps out oxygenated blood to the aorta. In order to investigate the effect of inertial forces

Table 1. Computation showing the coefficients of wall shear stress $G[n]$ for various values of viscosity variation parameter β

N	$\beta = 0$, G[n]	$\beta = -0.05$, G[n]	$\beta = -0.1$, G[n]
0	3.00000000000000	3.00000000000000	3.00000000000000
1	−0.34285714285714	−0.30535714285714	−0.26785714285714
2	−0.02345083487940	−0.35182977736549	−0.04372762059369
3	−0.00268009541478	−0.00440344667290	−0.00690190953816
4	−0.00034963897656	−0.00057383332687	−0.00103171741713
5	−0.00004866740259	−0.00007687414215	−0.00014547412140
6	$-0.7064052946 \cdot 10^{-5}$	−0.00001061052555	−0.00001957187484
7	$-0.1057210166 \cdot 10^{-5}$	$-0.1512047004 \cdot 10^{-5}$	$-0.2562038386 \cdot 10^{-5}$
8	$-0.1620051989 \cdot 10^{-6}$	$-0.2221646521 \cdot 10^{-6}$	$-0.331576840 \cdot 10^{-6}$
9	$-0.252966029 \cdot 10^{-7}$	$-0.335874907 \cdot 10^{-7}$	$-0.429626424 \cdot 10^{-7}$
10	$-0.4010840998 \cdot 10^{-8}$	$-0.5209280564 \cdot 10^{-8}$	$-0.5716366253 \cdot 10^{-8}$
11	$-0.6440269362 \cdot 10^{-9}$	$-0.8249779771 \cdot 10^{-9}$	$-0.8077109705 \cdot 10^{-9}$
12	$-0.1045178200 \cdot 10^{-9}$	$-0.1328333584 \cdot 10^{-9}$	$-0.1225257987 \cdot 10^{-9}$
13	$-0.171162579 \cdot 10^{-10}$	$-0.21671970 \cdot 10^{-10}$	$-0.199209425 \cdot 10^{-10}$
14	$-0.282497644 \cdot 10^{-11}$	$-0.357080701 \cdot 10^{-11}$	$-0.344904046 \cdot 10^{-11}$

Table 2. Computations showing the flow separation position and the bifurcation points using D-T method

β	0	−0.05	−0.1
Rd (turning points)	5.4581086861	5.269995742	5.154377742
Rd (separation)	4.712388903846	4.418569188	4.113917191

and the variable viscosity on the flow characteristics as well as the position of separation in the flow field, we expand G (i.e., the wall shear stress) in powers of Rd to obtain

$$G = 3 - \frac{3Rd}{140}\left(16 + \frac{35S\beta}{m}\right) - \frac{Rd^2}{862400}\left(20224 - 229845\frac{S\beta}{m} - 549780\frac{S^2\beta^2}{m^2}\right)$$
$$- \frac{Rd^3}{241472000}\left(647168 - 5760685\frac{S\beta}{m} + 58147320\frac{S^2\beta^2}{m^2} + 138091800\frac{S^3\beta^3}{m^3}\right) + \cdots \tag{38}$$

where $Rd = Re m$ i.e. the product of flow Reynolds number and arterial slope parameter. Without loss of generality, we let $x = (m-1)/m$ and compute the first 15 coefficients of the above series for different small values of viscosity variation parameter β, (see Table 1). The signs of the coefficients are the same and are monotonically decreasing in magnitude; hence the convergence of the series may be limited by a singularity on the positive real axis of Rd. Following [6], we seek a polynomial of degree $d \geq 2$, both in the dependent and independent variables (i.e. a special type of Hermite–Padé approximants) from the obtained partial sum given in order to analyse the solution structure of the problem. Let

$$F_d(Rd, G) = \sum_{m=1}^{d}\sum_{k=0}^{m} f_{m-k,k}\, Rd^{m-k} G^k \tag{39}$$

such that

$$\frac{\partial F_d}{\partial G}(0,0) = 1 \tag{40}$$

and

$$F_d(Rd, G) = O(Rd^{N+1}) \quad \text{as } Rd \to 0. \tag{41}$$

The requirement (41) reduces the problem to a system of N linear equations for the unknown coefficients of F_d. The entries of the underlying matrix depend on the N given coefficients of G. Henceforth we shall take

$$N = \frac{1}{2}(d^2 + 3D - 2), \tag{42}$$

so that the number of equations equals the number of unknowns. The bifurcations for the new polynomial can then be analysed locally by means of Newton's diagram. Details of bifurcation point classification are summarised in Chapter 2 of Drazin's book [5]. We compute the bifurcation points, the asymptotic behaviour of G as $Rd \to 0$ on the secondary solution branch and the Reynolds numbers at which separation occur in the flow field i.e. $G \to 0$, as shown in Table 2.

5. Graphical results and discussion

From our analysis, it is noteworthy that a negative increase in the value of β represents an increase in the blood viscosity. Figure 1 shows the transverse variation of blood axial velocity profile, a parabolic profile of Poiseuille flow is observed i.e. velocity is maximum at the arterial centreline and minimum at the walls. However, it is interesting to note that the blood moves faster when $\beta = 0$ as compare to the case when $\beta = -50, -100$. This can be attributed to a general increase in the blood viscosity.

Figure 2 shows the variation in the arterial wall shear stress. We observe a decrease in the wall shear stress with an increase in axial distance. This can be attributed to the diverging nature of the large arterial geometry under consideration. However, high wall shear stress at the arterial wall is observed when $\beta = -5, -10$ due to high blood viscosity, this may lead to early damage of the inner lining of the blood vessel i.e. the intima and the media. Figure 3 shows a sketch of the bifurcation diagram for the problem obtained using the D-T method for $\beta = 0, -0.05, -0.1$. Two major solution branches (I and II) are observed and a turning point exist between the two solutions. On the secondary solution branch $G \to -142.44828/Rd$ as $Rd \to 0$. Meanwhile, the magnitude of the bifurcation point together with the Reynolds number at which separation occur in the flow field decreases with an increase in the blood viscosity i.e. from $\beta = 0$ to -0.1, (see Table 2). Hence, an increase in the blood viscosity may preferentially cause early buildup of fat deposit at the stagnation zone of the blood vessel (separation position) that can eventually lead to the formation of a plague of atheroma [15].

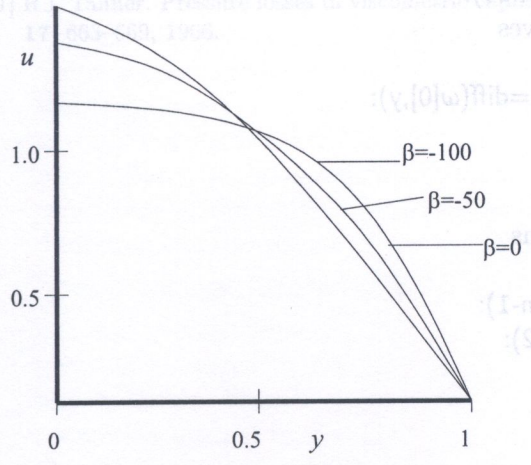

Fig. 1. Axial velocity profile of the flow, $Re = 1.0$, $x = 0.1$, $m = 0.01$

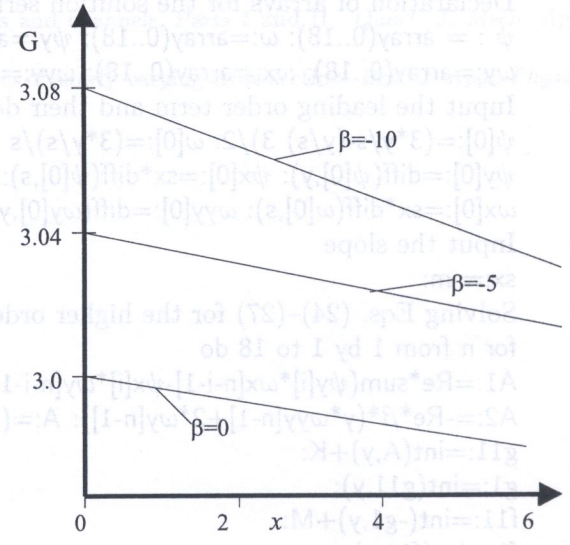

Fig. 2. Variation in wall shear stress with axial distance, $Re = 1.0$, $m = 0.01$

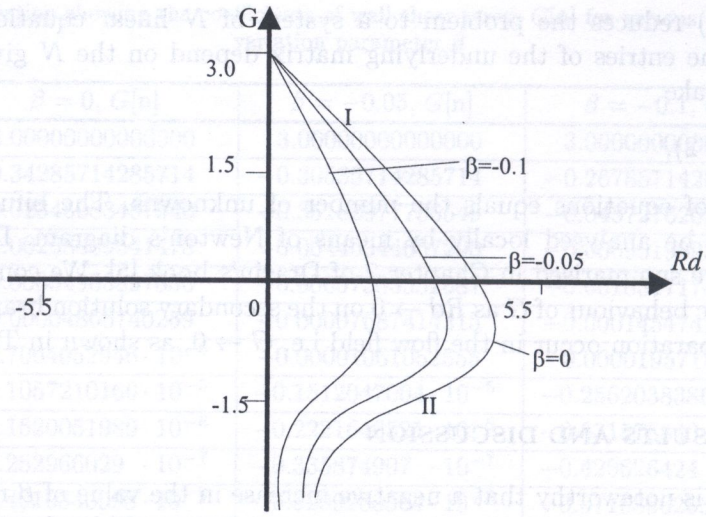

Fig. 3. A sketch of the bifurcation diagram for wall shear stress with Rd

6. Conclusion

The mathematical simulation of the arterial blood variable viscosity effect on the arteriosclerosis development is presented. The analysis reveals the existence of turning points in the flow field, however, a slight increase in blood viscosity may lead to early occurrence of flow separation in the blood vessel and subsequent the development of the atherosclerotic diseases. Finally, several factors like, high cholesterol diet, cigarette smoking, age, blood pressure, etc., can lead to elevated level of certain blood substances and thereby cause a rapid variation in the blood viscosity which may invariably lead to the. These events can increase the risk of heart attack or stroke.

Appendix

The MAPLE procedure to solve the system of equations (24)–(27) and the values of the coefficients of wall shear stress.

```
#   Declaration of arrays for the solution series coefficients
    ψ : = array(0..18): ω:=array(0..18): ψy:=array(0..18): ψx:=array(0..18):
    ωy:=array(0..18): ωx:=array(0..18): ωyy:=array(0..18):
#   Input the leading order term and their derivatives
    ψ[0]:=(3*y/s-(y/s) 3)/2: ω[0]:=(3*y/s)/s 2:
    ψy[0]:=diff(ψ[0],y): ψx[0]:=sx*diff(ψ[0],s): ωy[0]:=diff(ω[0],y):
    ωx[0]:=sx*diff(ω[0],s): ωyy[0]:=diff(ωy[0],y):
#   Input the slope
    sx:= m:
#   Solving Eqs. (24)–(27) for the higher order terms
    for n from 1 by 1 to 18 do
    A1:=Re*sum(ψy[i]*ωx[n-i-1]-ψx[i]*ωy[n-i-1],i=0..n-1):
    A2:=-Re*β*(y*ωyy[n-1]+2*ωy[n-1]): A:=(A1+A2):
    g11:=int(A,y)+K:
    g1:=int(g11,y):
    f11:=int(-g1,y)+M:
    f1:=int(f11,y):
    y:=s:
    K:=solve(f11=0,K): M:=solve(f1=0,M):
```

```
y:='y':
ψ[n]:=f1: ω[n]:=g1: ψy[n]:=diff(ψ[n],y): ψx[n]:=sx*diff(ψ[n],s):
ωy[n]:=diff(ω[n],y): ωx[n]:=sx*diff(ω[n],s): ωyy[n]:=diff(ωy[n],y):
K:='K': M:='M':
# Computing the wall shear stress coefficients
print(evalf(sub(y=s, ω[n]*ś2)));
od:
quit();
```

REFERENCES

[1] G.A. Baker Jr. *Essentials of Padé Approximants.* Academic Press, New York, 1975.

[2] G.K. Batchelor. *An Introduction to Fluid Dynamics.* Cambridge University Press, 1967.

[3] H. Blasius. Laminare Stromung in Kanalen wechselnder Breite. *Z. Math. Phys.*, **58**: 225–233, 1910.

[4] J.C.F. Chow, K. Soda. Laminar flow and blood oxygenation in channels with boundary irregularities. *J. Appl. Mech. (Trans. ASME)*, **40**: 843, 1973.

[5] P.G. Drazin. *Nonlinear Systems.* Cambridge University Press, 1992.

[6] P.G. Drazin, Y. Tourigny. Numerical study of bifurcation by analytic continuation of a function defined by a power series. *SIAM Journal of Appl. Math.*, **56**: 1–18, 1996.

[7] M. van Dyke. Computer-extended series. *Annual Rev. Fluid Mech.*, **16**: 287–309, 1984.

[8] J.A. Fox, A.E. Hugh. Localization of atheroma: a theory based on boundary layer separation. *Br. Heart J.*, **28**: 388–399, 1966.

[9] A.J. Lee. Blood viscosity related to risk of early atherosclerosis in men. *Circulation*, **97**: 1467–1473, 1998.

[10] M.J. Lighthill. Physiological fluid dynamics: A survey. *J. Fluid Mech.*, **52**: 475–497, 1972.

[11] R.D. Lucas. A perturbation solution for viscous incompressible flow in channels. Ph.D. dissertation, Stanford Univ., Stanford, Ca., USA, 1972.

[12] O.D. Makinde. Laminar flow in a channel of varying width with permeable boundaries. *Rom. J. Phys.*, **40**: 403–417, 1995.

[13] O.D. Makinde. Steady flow in a linearly diverging asymmetrical channel. *CAMES* **4**: 157–165, 1997.

[14] O.D. Makinde. Extending the utility of perturbation series in problems of laminar flow in a porous pipe and a diverging channel. *J. Austral. Math. Soc. Ser. B*, **41**: 118–128, 1999.

[15] O.D. Makinde. Effect of variable viscosity on arterial blood flow. *Far East J. Appl. Math.*, **4**(1): 43–58, 2000.

[16] M.J. Manton. Low Reynolds number flow in slowly varying axisymmetric tubes. *J. Fluid Mech.*, **49**: 401, 1971.

[17] D.A. McDonald. Steady flow in tubes of slowly varying cross-sections. *J. Appl. Mech.*, **4**: 475, 1978.

[18] T.J. Pedley. *The Fluid Mechanics of Large Blood Vessels.* Cambridge University Press, Cambridge, 1980.

[19] Ch. Peeyush, J.S.V.R. Krishna Prasad. Low Reynolds number flow in tubes of varying cross-section with absorbing walls. *J. Math. Phys. Sci.*, **26**: 19–36, 1992.

[20] F.T. Smith. Flow through constricted or dilated pipes and channels, Parts I and II. *Quart. J. Mech. Appl. Math.*, **29**: 343 and 365, 1976.

[21] R.I. Tanner. Pressure losses in viscometric capillary tubes of slowly varying cross-section. *Brit. J. Appl. Physics*, **17**: 663–669, 1966.